High-magnetic-field phase diagram of a quasi-one-dimensional metal

J. S. Qualls,[1] C. H. Mielke,[2] J. S. Brooks,[1] L. K. Montgomery,[3] D. G. Rickel,[2] N. Harrison,[2] and S. Y. Han[1]
[1]*NHMFL, Florida State University, Tallahassee, Florida 32310*
[2]*Los Alamos National Laboratory/NHMFL, MS E536, Los Alamos, New Mexico 87545*
[3]*Department of Chemistry, Indiana University, Bloomington, Indiana 47405*
(Received 4 February 2000; revised manuscript received 15 August 2000)

We report the high magnetic-field phase (to 45 T) of the quasi-one-dimensional organic conductor $(TMTSF)_2ClO_4$ in its thermally quenched phase. Termed ''Q-ClO_4,'' this phase exhibits a spin-density-wave (SDW) transition at ≈ 5 K which is strongly magnetic-field dependent, and distinct from the phase extensively studied in the annealed material. The field dependence of the SDW transition is well modeled by the theoretical treatment of Bjelis and Maki. We discuss the *B*-*T* phase diagram of Q-ClO_4 in the context of the hierarchy of low-dimensional organic metals (one-dimensional towards two-dimensional), and describe the temperature dependence of the quantum oscillations observed in the SDW phase.

Quasi-one-dimensional organic metals have the general character of a large bandwidth along the molecular stacking (chain) direction, followed by significantly smaller bandwidths in the interchain and interplane directions.[1] For the Bechgaard salts these ratios are (t_a, t_b, t_c: 1000, 250, 3 meV), respectively.[2] For sufficiently small transverse bandwidths, a one-dimensional conductor will undergo an instability, at a critical temperature, to an insulating ground state. Following Yamaji,[3] this temperature has an anisotropic bandwidth dependence in terms of the so-called ''imperfect nesting parameter,'' $\varepsilon_0 = t_b^2/t_a$. Hence the more two-dimensional the material is, the larger ε_0 will be, and the lower the temperature where the instability, or ''nesting'' will occur. In the case of the Bechgaard salts, a spin-density wave (SDW) ground state is formed. For sufficiently large ε_0, the low-temperature ground state remains metallic, but high magnetic fields can effectively reduce ε_0 (i.e., drive the system more one-dimensional), and a field-induced spin-density wave state (FISDW) can be stabilized.[4] This latter phenomena has been the subject of extensive experimental and theoretical work.[1]

In this paper we consider a system where ε_0 is large, but where an SDW state still forms at a temperature $T_{SDW} = 5$ K. This allows a unique situation where T_{SDW} increases by a factor of 2 in high magnetic fields due to the close competition between ε_0 and the magnetic energy. To accomplish this we employ the well-studied organic conductor $(TMTSF)_2ClO_4$.[1] What is particular to our approach is that the material has been prepared in a very rapidly (30 K/s) thermally quenched state (i.e., Q-ClO_4) to preserve the high-temperature electronic structure, which is comprised of two, open orbit, warped Fermi surface sheets. Otherwise, if the material is slowly cooled, the tetrahedral anion ClO_4 undergoes an ordering transition around 24 K, the unit cell doubles in the *b* direction, and the resulting Fermi surface becomes more complex.[5] Generally, it is this relaxed state of the material (hereafter R-ClO_4), which has been most extensively studied. In contrast, Q-ClO_4 is in the class of Bechgaard salts[2,6] $(TMTSF)_2X$ where $X = PF_6$, AsF_6, NO_3 which form an SDW state at ambient pressure below a transition temperature T_{SDW} (12 K for $X = PF_6$ and AsF_6, 10 K for $X = NO_3$, and 5 K for $X =$ Q-ClO_4). In these cases a high magnetic field improves the nesting condition,[7–9] and T_{SDW} increases with magnetic-field. This field effect was first predicted theoretically by Montambaux.[10] We present in this paper the field dependence of T_{SDW} for Q-ClO_4 where the effect is very dramatic, and exhibits a *B*-*T* phase diagram in the hierarchy of nesting parameters ($7\ \text{K} \leqslant \varepsilon_0 \leqslant 22.5$ K) in the Bechgaard salts. We note two early, independent reports of the magnetic-field dependence of the field dependence of T_{SDW} for Q-ClO_4, one in pulsed fields[11] to 50 T, and another[12] to 27 T. Both considered the theoretical framework of Bjelis and Maki,[13] as discussed below.

The measurements reported here were carried out on two samples in 50 T (sample 1) and 60 T (sample 2) pulsed-field magnets at the Los Alamos National Laboratory. Electrical transport contacts were made via graphite paint and 12 μm gold wires, with a dc four-terminal technique with a current of 50 μA. The current was applied transverse to the layers along the *c* axis, as were the voltage contacts. The magnetic-field is also along the *c* axis. To ensure that the samples fully quenched, the samples were put in direct contact with liquid-helium from room temperature as rapidly as possible. Estimated cooling rates were of order 30 K/s or greater. The use of graphite paint appeared to greatly enhance the reliability of the contacts and to reduce degradation (cracking) of the samples during the rapid cooldowns. Systematic temperature measurements for each run were performed with a single quench to preserve the anion disorder in the samples.

In Fig. 1(a) we show a summary of the magnetoresistance measurements for sample 1 above 5 K, and in Fig. 1(b) similar measurements at lower temperatures for both samples 1 and 2 are presented. In the inset of Fig. 1(a) the temperature dependence of the *c*-axis resistivity is shown at zero magnetic-field. Here the upturn is the onset of the spin-density-wave transition, as established by, for instance NMR studies.[6] In Fig. 2 we show an expanded view of the behavior of the magnetic-field-dependent resistance, where the data has been plotted vs the square of the magnetic-field. All data shown is for temperatures higher than T_{SDW} ($B = 0$). Here

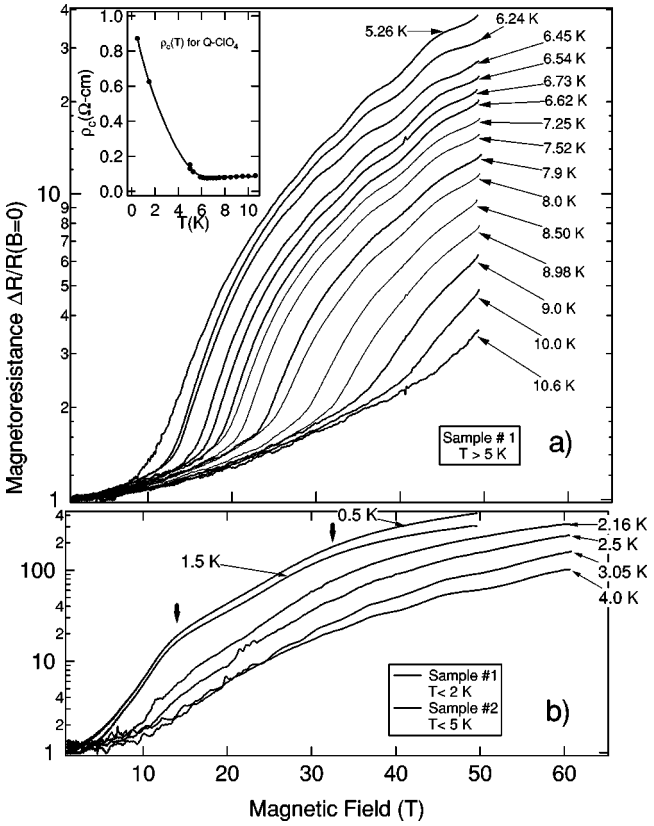

FIG. 1. (a) Magnetoresistance $\Delta R/R(B=0)$ of thermally quenched $(TMTSF)_2ClO_4$ vs pulsed magnetic field above 5 K (sample 1). Inset: zero-field *c*-axis resistivity vs temperature. (b) Low-temperature magnetoresistance vs pulsed magnetic field for samples 1 and 2. Arrows indicate the position of structure in the lowest temperature data (see text).

the magnetoresistance remains small, and quadratic in field, until a critical field (hereafter B_{SDW}) is reached. We have fit the 10.6 K resistance data in Fig. 2 to the quadratic function (expected for the case of an open orbit metal) below the point where the slope changes. Aside from a weak temperature dependence, all of the data follow this general functional dependence until the point B_{SDW} is reached. B_{SDW} is temperature dependent, and is manifested as a change in the field dependence of the magnetoresistance. This defines the threshold field between the metallic and SDW ground states. Above B_{SDW}, additional structure appears (hereafter B'_{SDW}) where the field dependence of the magnetoresistance changes again. At higher fields quantum oscillations of frequency $F = 190$ T become evident. We will return to these last two points in the discussion below.

In Fig. 3 we summarize the dependence of B_{SDW} and B'_{SDW} in terms of the corresponding temperatures T_{SDW} and T'_{SDW} based on the analysis of Fig. 2 and the zero-field value from the inset of Fig. 1(a). The new phase diagram, as defined by Fig. 3, is the main result of the present work. To put the new data for Q-ClO_4 in perspective, we have included previous results for AsF_6, PF_6, and NO_3, (Refs. 7,8,14) for the field dependence of T_{SDW} in terms of the theoretical framework Bjelis and Maki[13] (see also earlier work of Montambaux[10]) which describes the magnetic-field dependence of T_{SDW} in the form

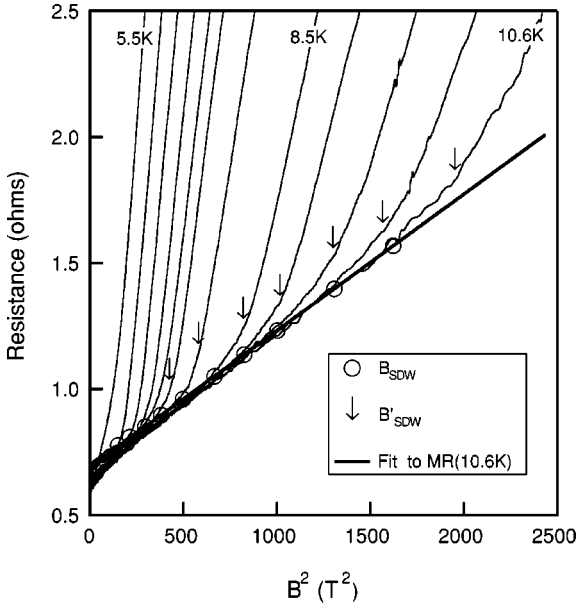

FIG. 2. Detail of the resistance of sample 1 vs the square of the magnetic field for different temperatures. The solid line is a fit of the high-temperature (10.4 K) resistance to a quadratic field dependence. B_{SDW} (T_{SDW}) is defined as the point of deviation of the resistance from a quadratic behavior in field (open circles), and B'_{SDW} (T'_{SDW}) is a second change in the field dependence (see arrows) of the resistance at higher fields. (Complete temperature labels, left to right, are 5.5, 6.45, 6.5, 6.54, 7.25, 7.52, 7.90, 8.5, 8.98, 9.0, 10.0, and 10.6 K.)

$$\ln\left[\frac{T_{\mathrm{SDW}}}{T_{\mathrm{SDW0}}}\right] \cong \sum_{l=-\infty}^{\infty} J_l^2(e_0)\left\{\mathrm{Re}\,\Psi\left(\frac{1}{2}+2ilx_1\right)-\Psi\left(\frac{1}{2}\right)\right\}. \tag{1}$$

Here $e_0=\varepsilon_0/\omega_b$, where ε_0 is the imperfect nesting parameter described above, and $\omega_b=ev_F bB$. The latter is the effective cyclotron frequency along the *b* axis, where v_F is the Fermi velocity. J_l and Ψ are Bessel and digamma functions, respectively, and $x_1=\omega_b/4\pi T_{\mathrm{SDW}}$. T_{SDW0} corresponds to the transition temperature for perfect nesting. This expression, in an asymptotic form,[7] successfully describes the field dependence of T_{SDW} for $(TMTSF)_2NO_3$ Ref. 7 and $(TMTSF)_2PF_6$ Ref. 9. For Q-ClO_4, Eq. (1) is also applied, but its full (nonasymptotic) form must be used to obtain proper convergence at low magnetic fields due to the large imperfect nesting parameter ε_0 needed to describe the data. The fitting parameters for all three materials are listed in the caption of Fig. 3. It is clear that T_{SDW} (B =0) decreases with increasing ε_0. However, since the general Fermi surface topology is very similar, all three materials approach a common transition temperature in the high-field limit. Of note is that v_F for Q-ClO_4 is half that of the other two materials, but this value produced the best fit to the experimental data. At this point we cannot tell if this is due to details of the theoretical model vs the data, or if the value of v_F obtained reflects slight changes in the band structure of the ClO_4 material in the quenched state (e.g., see discussion of ''RO'' frequencies below).

For completeness, the phase diagram of R-ClO_4 is also shown[5] in Fig. 3. A point that must be clearly made is that the Q-ClO_4 phase diagram is very different from that studied

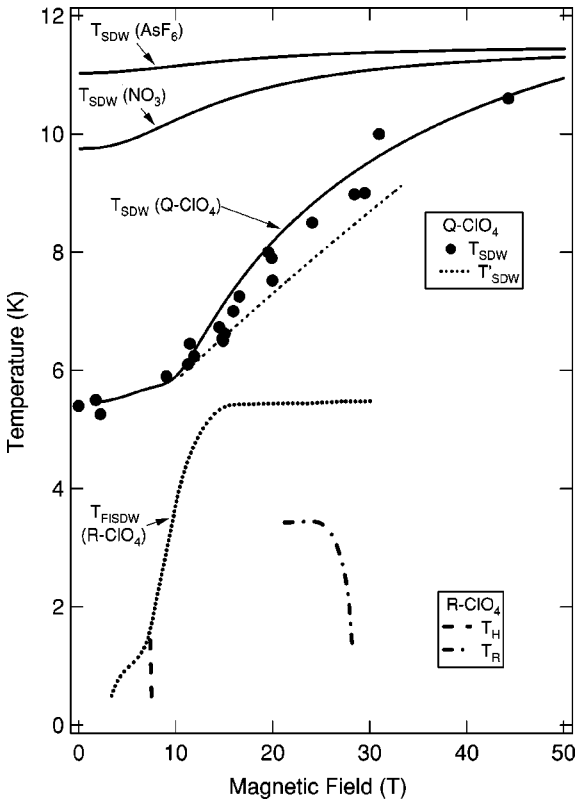

FIG. 3. Temperature vs magnetic-field phase diagram of Q-ClO_4 based on the values of T_{SDW} vs B_{SDW} (also T'_{SDW} vs B'_{SDW}) obtained from Fig. 2. The solid lines are fits of the theoretical expression of Bjelis and Maki from Eq. (1) with the parameters v_F, T_0, and ε_0 for $X=AsF_6$ ($v_F=2.4\times10^5$ m/s; $\varepsilon_0=7$ K; $T_0=11.5$ K), $X=NO_3$ ($v_F=2.4\times10^5$ m/s; $\varepsilon_0=13$ K; $T_0=11.0$ K), and $X=$Q-ClO_4 ($v_F=1.1\times10^5$ m/s; $\varepsilon_0=22.5$ K; $T_0=13.0$ K; see text for discussion of v_F). The dashed line is a polynomial fit to T'_{SDW} vs B'_{SDW}. The lower phase diagram is for R-ClO_4 after Ref. 5. The finely dashed line is the main second-order phase boundary between the metallic and FISDW phases. The other two phase lines T_H and T_R delineate subphases (see Ref. 5).

in the R-ClO_4 case. For R-ClO_4 the Fermi surface topology involves double open orbit sheets due to the anion ordering, the imperfect nesting is so large that at zero field the system is metallic, even superconducting ($T_c=1.2$ K), and the maximum field-induced T_{SDW} is less than 6 K. Another factor which distinguishes Q-ClO_4 from R-ClO_4 is that the quantum oscillation frequency in the magnetoresistance is 190 T, as confirmed by this (see below) and previous independent studies.[9] In contrast, for R-ClO_4 the frequency is 250 T. This confirms that the Fermi surface topologies are fundamentally different. Returning for a moment to the observation of the B'_{SDW} feature (Figs. 2 and 3), it is not clear what assignment to make to it (i.e., a SDW subphase for instance). It falls outside the prediction of Eq. (1) since there only one transition (B_{SDW}) is predicted. Hence further experimental and theoretical work will be needed to fully understand the significance of B'_{SDW}.

We next turn to the nature of the oscillations in the magnetoresistance which appear above B_{SDW} (see Fig. 1). The oscillatory component of the magnetoresistance, plotted as $\Delta R/R$ vs inverse magnetic field is shown in Figs. 4(a) and 4(b) for representative temperatures. (Here R is the nonoscillatory background magnetoresistance.) The oscillation amplitude increases until about 5 K, but then rapidly vanishes at lower temperatures. In Fig. 4(c) we show the amplitude of the oscillations (normalized by R) as a function of temperature. Such oscillations, commonly called ''rapid oscillations'' or ''RO'' appear in a number of the quasi-one-dimensional organic salts, including the Bechgaard salts[1] and the $(DMET\text{-}TSeF)_2AuCl_2$ salts.[15] These oscillations are pe-

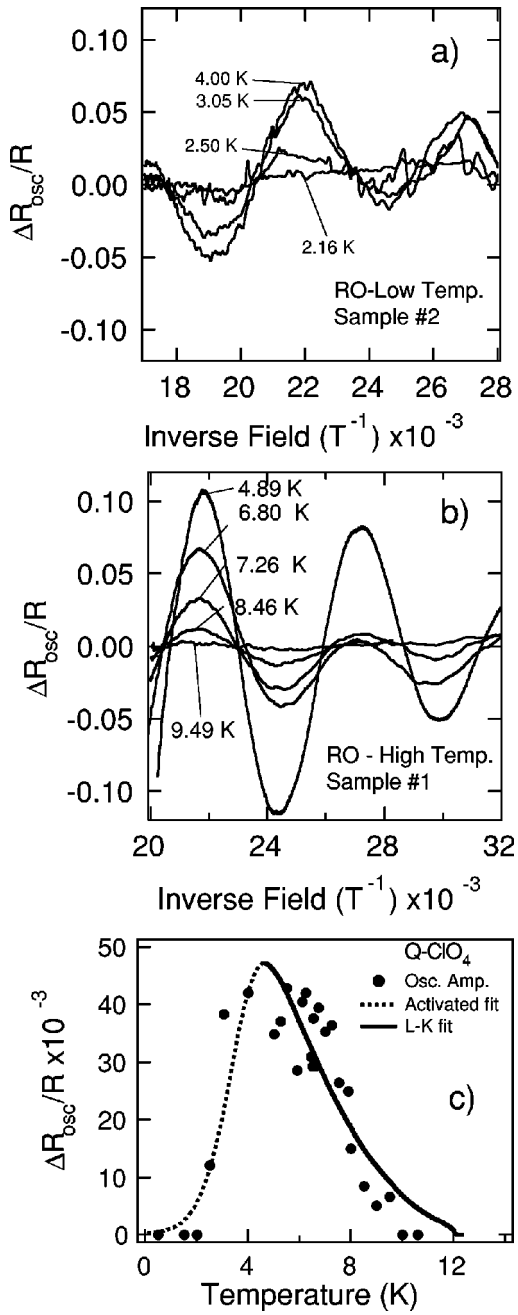

FIG. 4. Temperature dependence of the quantum oscillations (normalized by the background magnetoresistance). The frequency is 190 ± 5 T. (a) Low-temperature behavior (sample 2) below 5 K. (b) High-temperature behavior (sample 1) above 5 K. (c) Plot of the amplitudes vs temperature in the range 30 to 50 T for both samples measured. The solid line is a fit of the data to the standard Lifshitz-Kosevich formula for quantum oscillation amplitudes above T^* ($=3.75$ K), and to an activated behavior (dashed line) below T^* (see text).

riodic in inverse field, with a frequency of between 190 and 250 T. If considered as closed orbits, they represent about 3% of the first Brillouin zone. A general observation is that they only occur when the original open orbit Fermi surface has undergone a reconstruction. This can happen by an anion ordering transition[16] and/or nesting of the Fermi surface.[9] In many cases where a spin-density-wave ground state is stabilized, the amplitude of the rapid oscillations first increases with decreasing temperature, but below a characteristic temperature T^* (typically between 2 and 4 K), the amplitude attenuates exponentially for $T \rightarrow 0$. These oscillations have been described as a magnetic breakdown phenomena[9] in an imperfectly nested Fermi-surface topology. However, below T^* there is an improvement of the nesting condition, such that more of the reconstructed Fermi surface becomes gapped, and the magnetic breakdown becomes less probable. As shown in Fig. 4(c), and following Ref. 9, this behavior may be modeled by the standard Lifshitz-Kosevich description for quantum oscillations above T^*, and an exponential attenuation below T^*. Here the parameters of the model involve an effective mass $m^* = 1.2\ m_0$, a Dingle temperature $T_D = 7$ K, a $T^* = 3.75$ K, and a low-temperature magnetic breakdown gap of 10 K.

The Dingle temperature associated with the quantum oscillations discussed above gives insight into the nature of carrier scattering, and therefore disorder, in Q-ClO_4. Typically for ''clean'' organic metals where strong quantum oscillations are observed,[17] T_D is of order 1 K. For Q-ClO_4 it is considerably higher (7 K). Since anion disorder is necessary to stabilize the Q-ClO_4 state, this could be a possible source for the enhanced scattering. However, similar studies of the quantum oscillations in AsF_6 and PF_6 anion systems,[9] where there is no disorder involved, show a similar value of T_D. Furthermore, given that the SDW state, which should be sensitive to disorder, readily develops in Q-ClO_4, we speculate that in spite of the anion disorder, the material is in some sense still relatively clean, and the large value of T_D may be characteristic of the SDW (antiferromagnetic) nature of these systems.

One other feature of the low-temperature data is shown in Fig. 1(b). Below about 3 K there are two distinct changes (shown by the arrows) in the magnetoresistance, one at around 12 T, and the other around 30 T. At present we have no explanation for these features. One possibility is that this behavior is related to the T^* mechanism in some manner. Another is that these changes are some vestige of the anion-ordered state that only shows up when the resistivity of the predominantly quenched state is sufficiently high. (The characteristic fields are close to some of the major FISDW phase boundaries in the R-ClO_4 compound.[18])

In summary, the present work shows the evolution of the metal-to-spin-density-wave transition for open orbit, quasi-one-dimensional metals with changes in their nesting parameters. By mapping the magnetic-field dependence of the spin-density-wave transition, we provide a description of the field-dependent ground state of the material $(TMTSF)_2ClO_4$ where its low-temperature anion ordering transition has been suppressed. The theory of Bjelis and Maki provide an excellent framework to describe the general field-dependent features of these systems. New aspects of the Q-ClO_4 ground state include the full description of the temperature dependence of the quantum oscillations in the spin-density-wave phase, which attenuate exponentially below 5 K, and a nearly quadratic field dependence of the resistance in the lower field, high-temperature metallic phase of the system. Some evidence is also present for additional subphase structure in the B-T phase diagram, but further work will be needed to make accurate assignments to these features.

We are indebted to K. Maki for testing the convergence of Eq. (1) at low fields, and to D. Agterberg who gave us valuable advice on the computation involved. Support from NSF-DMR 95-10427 and 99-71474 (J.S.B.) and a cooperative agreement between NSF-DMR95-27035 and the State of Florida (NHMFL) is acknowledged.

[1] T. Ishiguro, G. Saito and K. Yamaji, *Organic Superconductors*, 2nd ed. (Springer, Berlin, 1998).
[2] K. Bechgaard, C.S. Jacobsen, K. Mortensen, H.J. Pedersen, and N. Thorup, Solid State Commun. **33**, 1119 (1980).
[3] K. Yamaji, J. Phys. Soc. Jpn. **51**, 2787 (1982).
[4] L.B. Gor'kov and A.G. Lebed', J. Phys. (France) Lett. **60**, 1189 (1984). This is the so-called ''standard model'' for FISDW formation. See also Ref. 7 in Ref. 18 below.
[5] S.K. McKernan, S.T. Hannahs, U.M. Scheven, G.M. Danner, and P.M. Chaikin, Phys. Rev. Lett. **75**, 1630 (1995).
[6] J.M. Delrieu, M. Roger, Z. Toffano, A. Moradpour, and K. Bechgaard, J. Phys. (Paris) **47**, 839 (1986).
[7] A. Audouard and S. Askenazy, Phys. Rev. B **52**, 700 (1995).
[8] S. Uji, J.S. Brooks, M. Chaparala, S. Takasaki, J. Yamada, and H. Anzai, Phys. Rev. B **55**, 12 446 (1997).
[9] J.S. Brooks, J. O'Brien, P.R. Starrett, R.G. Clark, S.Y. Han, J.S. Qualls, S. Takasaki, J. Yamada, H. Anzai, C.H. Mielke, and L.K. Montgomery, Phys. Rev. B **59**, 2604 (1999).
[10] The field dependence of T_{SDW} was treated for $(TMTSF)_2PF_6$ by G. Montambaux, Phys. Rev. B **38**, 4788 (1988), where a phase diagram very similar to that in Fig. 3 was predicted.
[11] C.H. Mielke, N. Harrison, J.C. Cooley, J.D. Goettee, D.J. Rickel, L.K. Montgomery, M.M. Honold, and J.S. Brooks, Bull. Am. Phys. Soc. **44**, 1165 (1999).
[12] T. Matsunga *et al.*, J. Phys. IV **9**, 210 (1999).
[13] A. Bjelis and K. Maki, Phys. Rev. B **45**, 12 887 (1992).
[14] M.J. Naughton, J.P. Ulmet, I.J. Lee, and J.M. Fabre, Synth. Met. **85**, 1531 (1997).
[15] N. Biskup, J.S. Brooks, R. Kato, and K. Oshima, Phys. Rev. B **60**, R15 (1999).
[16] S. Uji, J.S. Brooks, S. Takasaki, J. Yamada, and H. Anzai, Solid State Commun. **103**, 387 (1997).
[17] J. Wosnitza, *Fermi Surfaces of Low Dimensional Organic Metals and Superconductors* (Springer-Verlag, Berlin, 1996).
[18] W. Kang, S.T. Hannahs, and P.M. Chaikin, Phys. Rev. Lett. **70**, 3091 (1993).